ACS SyntheticBiology

Research Article

pubs.acs.org/synthbio

A Versatile Microfluidic Device for Automating Synthetic Biology

Steve C. C. Shih,*[,†,‡] Garima Goyal,[†,§,∥] Peter W. Kim,[†,‡] Nicolas Koutsoubelis,[§,∥,#] Jay D. Keasling,[§,∥,⊥] Paul D. Adams,[†,∥] Nathan J. Hillson,[†,§,∥] and Anup K. Singh*[,†,‡]

[†]Technology Division, [§]Fuels Synthesis Division, Joint BioEnergy Institute, 5855 Hollis Street, Emeryville, California 94608, United States

[‡]Sandia National Laboratories, 7011 East Avenue, Livermore, California 94550, United States

[∥]Physical Bioscience Division, Lawrence Berkeley National Laboratory, 1 Cyclotron Road, Berkeley, California 94720, United States

[⊥]Department of Chemical & Biomolecular Engineering, Department of Bioengineering, University of California, Berkeley, California 94720, United States

Supporting Information

ABSTRACT: New microbes are being engineered that contain the genetic circuitry, metabolic pathways, and other cellular functions required for a wide range of applications such as producing biofuels, biobased chemicals, and pharmaceuticals. Although currently available tools are useful in improving the synthetic biology process, further improvements in physical automation would help to lower the barrier of entry into this field. We present an innovative microfluidic platform for assembling DNA fragments with 10× lower volumes (compared to that of current microfluidic platforms) and with integrated region-specific temperature control and on-chip transformation. Integration of these steps minimizes the loss of reagents and products compared to that with conventional methods, which require multiple pipetting steps. For assembling DNA fragments, we implemented three commonly used DNA assembly protocols on our microfluidic device: Golden Gate assembly, Gibson assembly, and yeast assembly (i.e., TAR cloning, DNA Assembler). We demonstrate the utility of these methods by assembling two combinatorial libraries of 16 plasmids each. Each DNA plasmid is transformed into *Escherichia coli* or *Saccharomyces cerevisiae* using on-chip electroporation and further sequenced to verify the assembly. We anticipate that this platform will enable new research that can integrate this automated microfluidic platform to generate large combinatorial libraries of plasmids and will help to expedite the overall synthetic biology process.

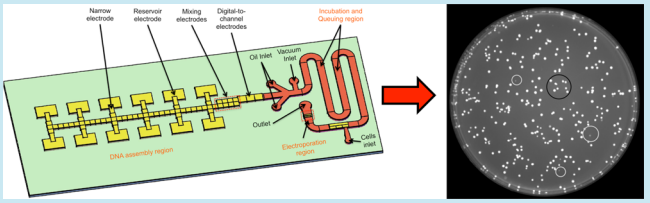

KEYWORDS: *digital microfluidics, droplet microfluidics, synthetic biology, DNA assembly, Golden Gate assembly, Gibson assembly, yeast assembly, TAR cloning*

In recent years, synthetic biology has become an approach to understand and to manipulate biological systems, including bacteria and yeast, for the production of biofuels, biobased chemicals, and pharmaceuticals.[1−5] However, given this extremely challenging goal, the biological design cycle for synthetic biology (specify−design−build−test−learn) is often very slow, expensive, and laborious.[6,7] To expedite this process, significant efforts are needed to develop enabling technologies for rapid biological engineering (e.g., an automated platform for building designs and testing the constructs in a host organism). Currently, there are many automation algorithms and software packages that expedite the *specification* and *design* processes[8−20] for the construction of biological circuits and metabolic pathways.[21,22] For the next two steps, *build* and *test*, there are currently automation tools to aid these processes,[23−26] but these steps are still relatively underserved in terms of physical automation technologies to build and test DNA assemblies. The addition of more physical automation technologies will help to lower the barrier of entry into this field. Construction of novel plasmids typically starts by obtaining DNA fragments and assembling them into plasmids. There are a variety of assembly methods, such as Gibson,[27] Golden Gate,[28,29] and yeast assembly (i.e., TAR cloning[30] or DNA Assembler[31]), that are commonly used for constructing new plasmids. For testing, fluorescent proteins can provide a convenient tool for characterizing expression,[32] and, frequently, colony PCR screening followed by Sanger or Next-Gen sequencing[23] is used to validate the sequences of the constructed plasmids. Currently, there are automation programs that can significantly reduce error rates and manual planning by optimizing assembly sequence and strategy and that have the potential to be integrated with other systems (e.g., robotics) to automate the whole process.[15,25,33,34] Robotic technology is expensive, however, and the consumable costs (plates, pipet tips, chemicals, cuvettes, etc.) can make assays costly. For example, the cost for materials and hands-on time for DNA assembly and cloning utilizing traditional liquid-handling robotic automation is estimated to be ∼$141 000 to synthesize 13 824 constructs.[9]

Received: March 29, 2015
Published: June 15, 2015

DOI: 10.1021/acssynbio.5b00062
ACS Synth. Biol. 2015, 4, 1151−1164

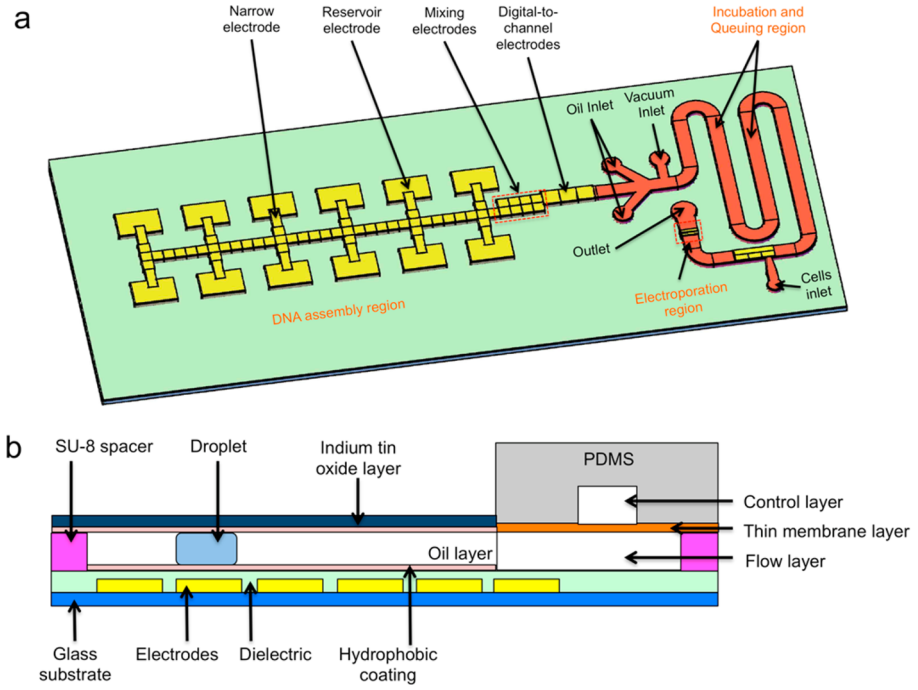

Figure 1. Microfluidic device for automating synthetic biology. (a) Schematic of the device, which comprises a bottom plate with patterned electrodes (shown in yellow) and a channel (shown in orange) to incubate droplets created by DMF and to electroporate cells with the assembled plasmid. Top-plate for DMF and top PDMS layer for the channel are not shown for clarity. (b) Side view of the device showing the digital-to-droplet interface (not to scale).

Process automation is quickly progressing from luxury to necessity, as target applications increasingly demand the fabrication of large combinatorial DNA libraries in the search for better antibodies, faster enzymes, and more productive microbial strains. Beyond the construction of the DNA libraries, inserting these plasmids into a microbial strain remains a major scale-limiting bottleneck in terms of both cost and time. Therefore, new physical automated technologies in synthetic biology are required to assemble and transform the construction of DNA part variations. By integrating these functions on one automated platform, it will help to accelerate the synthetic biology cycle.

Microfluidics, a lab-on-a-chip technology based on interconnecting, micron-dimension channels, is a format to study and manipulate small volumes of liquids on nanoliter (or even smaller) scales. The advantages of decreasing the scale allows for a more predictable fluid flow, a decrease in the volume of reagents needed for reactions, smaller device footprint, and integration with automation. Recently, synthetic biologists have been developing and using microfluidics to study gene networks and expression,[35] to multiplex gene synthesis,[36−38] and to detect intra/extracellular metabolites.[39] These cheap devices (~$5−10 per device) are made using networks of microchannels, which are suitable platforms for storing and driving small volumes of liquid and droplets (a paradigm called droplets-in-channel microfluidics).[40−44] Although microchannels and droplets-in-channel microfluidics are characterized by low reagent use, they are serial in nature and may not be well-suited for controlling many different reagents simultaneously. An alternative to these paradigms has recently emerged, called digital microfluidics (DMF).[45,46] As DMF is inherently an array-based technology, it is a natural fit for integrating fluid handling for applications requiring multiplexing.[47−49] In addition, in contrast to microchannels and droplets-in-channel microfluidics, digital microfluidics enables facile control over many different reagents simultaneously on-demand. Here, in response to the challenge described above, we propose to develop a hybrid (integrating both DMF and droplets-in-channel microfluidics) microfluidic platform that will harness the advantages of both systems to integrate the various molecular biology steps. Below, we describe an automated microfluidic-driven synthetic biology device that will build two sets of 16 plasmids using three DNA assembly methods and transform them into bacteria or yeast, which is further sequenced off-chip.

RESULTS AND DISCUSSION

Microfluidic DNA Assembly. In this work, we designed a microfluidic chip to automate processes required for synthetic biology. The 75 × 25 mm microfluidic device consisted of three distinct functional regions: DNA assembly, queuing and incubation, and transformation (Figure 1a). This microfluidic device consists of combining two paradigms of microfluidics, namely, digital and droplet microfluidics. The hybrid microfluidics technique (i.e., droplet-to-digital or digital-to-microchannel) has been used previously,[50−52] but this is the first digital-to-droplet microfluidic hybrid technique used for synthetic biology. The integration of synthetic biology with microfluidics requires liquids to be dispensed reproducibly from reservoirs into subdroplets. Dispensing liquid with digital microfluidics is highly reproducible and precise, and with feedback and impedance, we can obtain ~1.5% volumetric precision variation for six successive dispensed droplets (see Supporting Information Figure S1).

The DNA assembly region of the device consists of a digital microfluidic device with 76 electrodes (with interelectrode gaps of 20 μm), which includes 12 (3.6 × 3.0 mm) reservoir electrodes, 12 (2.5 × 1 mm) narrow electrodes (used for 100%

DOI: 10.1021/acssynbio.5b00062
ACS Synth. Biol. 2015, 4, 1151−1164

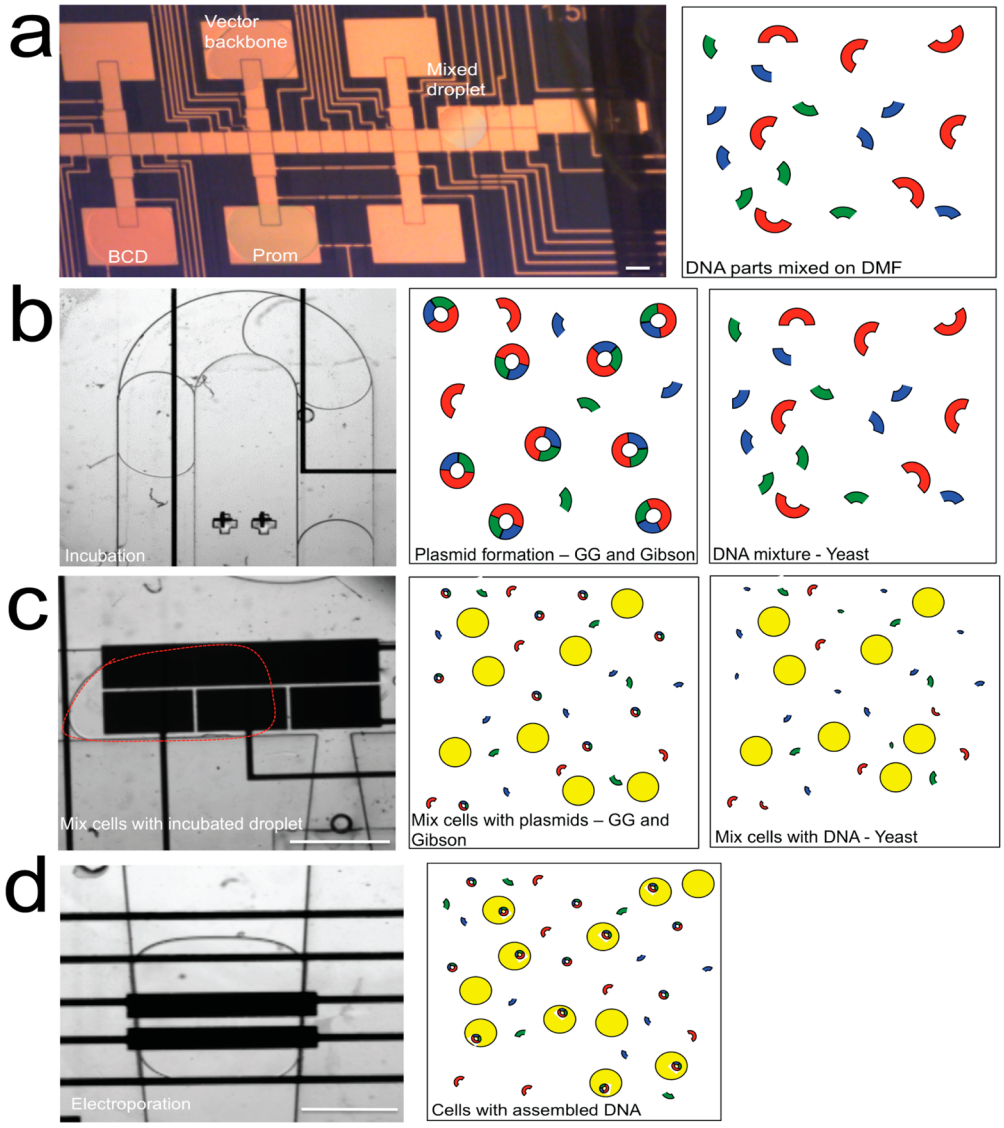

Figure 2. DNA assembly and electroporation. Frames from a movie (left) with a corresponding schematic showing a simplified DNA assembly mechanism (right). First, (a) droplets containing DNA fragments (i.e., vector backbone, promoter, BCD-gfp) are dispensed, mixed, and actuated to the channel. DNA ligase (for Golden Gate assembly) and 2× Gibson master mix (for Gibson assembly) are also added to the mixture (not shown). No additional droplets are necessary for yeast assembly. (b) The droplets are incubated in the channel for X min at Y (X = 10 − Golden Gate and yeast, 15 − Gibson; Y = 25 °C − Golden Gate and yeast, 50 °C − Gibson). After incubation, some plasmids are formed for Golden Gate and Gibson assembly, whereas for yeast assembly, plasmid formation occurs after transformation. (c) The assembled plasmid is mixed with cells (shown as the red outline) and is electroporated (d) by sending DC pulses to one microelectrode while grounding the other microelectrode. Scale bars, (a) 1 mm, (b, c) 1.5 mm, and (d) 1 mm.

dispensing fidelity, as shown from other studies[47,48]), eight (1.2 × 1.2 mm) mixing electrodes, three (1.75 × 1.75 mm) digital-to-channel electrodes, and 41 (1.2 × 1.2 mm) actuation electrodes (Figure 1a). Devices were assembled with an unpatterned ITO-glass top plate such that the top plate was flush against the side of the PDMS (Figure 1b). These two plates are separated by the SU-8 spacer, which has a thickness of ∼140 μm. With these dimensions, droplets covering the reservoir electrodes contained volumes of 1.5 μL, and droplets dispensed from reservoirs have volumes of ∼0.2 μL. After dispensing and mixing the necessary droplets (see Methods for a description of which droplets are dispensed and mixed) (Figure 2a), the droplets were introduced to the incubation and queuing part of the device consisting of a 1.5 mm wide serpentine channel. There are two inlets for the oil phase to drive droplet flow and one syringe-vacuum inlet to bring the droplet from the digital microfluidic device into the channel (Figure 2b). This serpentine channel has the capability to store 16 droplets and has the capability to store droplets for over 2 h without loss of volume. This region is also equipped with four valves (Supporting Information Figure S2) that control (1) the entrance of the mixed droplet from the digital microfluidic device (labeled as 1), (2) the oil inlets (labeled as 2 and 3), and (3) the entrance of the serpentine incubation channel to store droplets (labeled as 4). The electroporation region consists of one inlet for the bacteria or yeast suspension and an outlet for the droplets containing the transformed microbes. This region also consists of four electrodes (three 1.4 × 0.7 mm and one 4.0 × 0.7 mm) at the intersection of the cell inlet and the main channel. These are used to dispense droplets of cells and mix

DOI: 10.1021/acssynbio.5b00062
ACS Synth. Biol. 2015, 4, 1151−1164

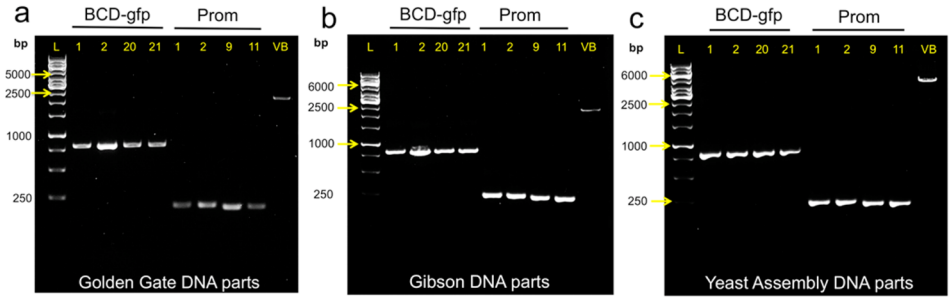

Figure 3. Gel electrophoresis (1%) images of the DNA fragments used for assembly. For (a) Golden Gate assembly, DNA parts were BsaI and DpnI digested and gel purified. For (b) Gibson assembly and (c) yeast assembly, parts were DpnI digested at 37 °C for 1 h and gel purified. BCD-gfp (1, 2, 20, 21) shows a band at ∼800 bp; promoter (1, 2, 9, 11) shows a bands at ∼100 bp. The Golden Gate and Gibson assembly vector backbone shows a band at ∼2100 bp, and the yeast assembly vector backbone shows a band at ∼5600 bp. Lane abbreviations: L, 1 kb DNA ladder (Fisher Scientific) for Golden Gate; L, 1 kb plus DNA ladder (Fisher Scientific) for Gibson and yeast assembly.

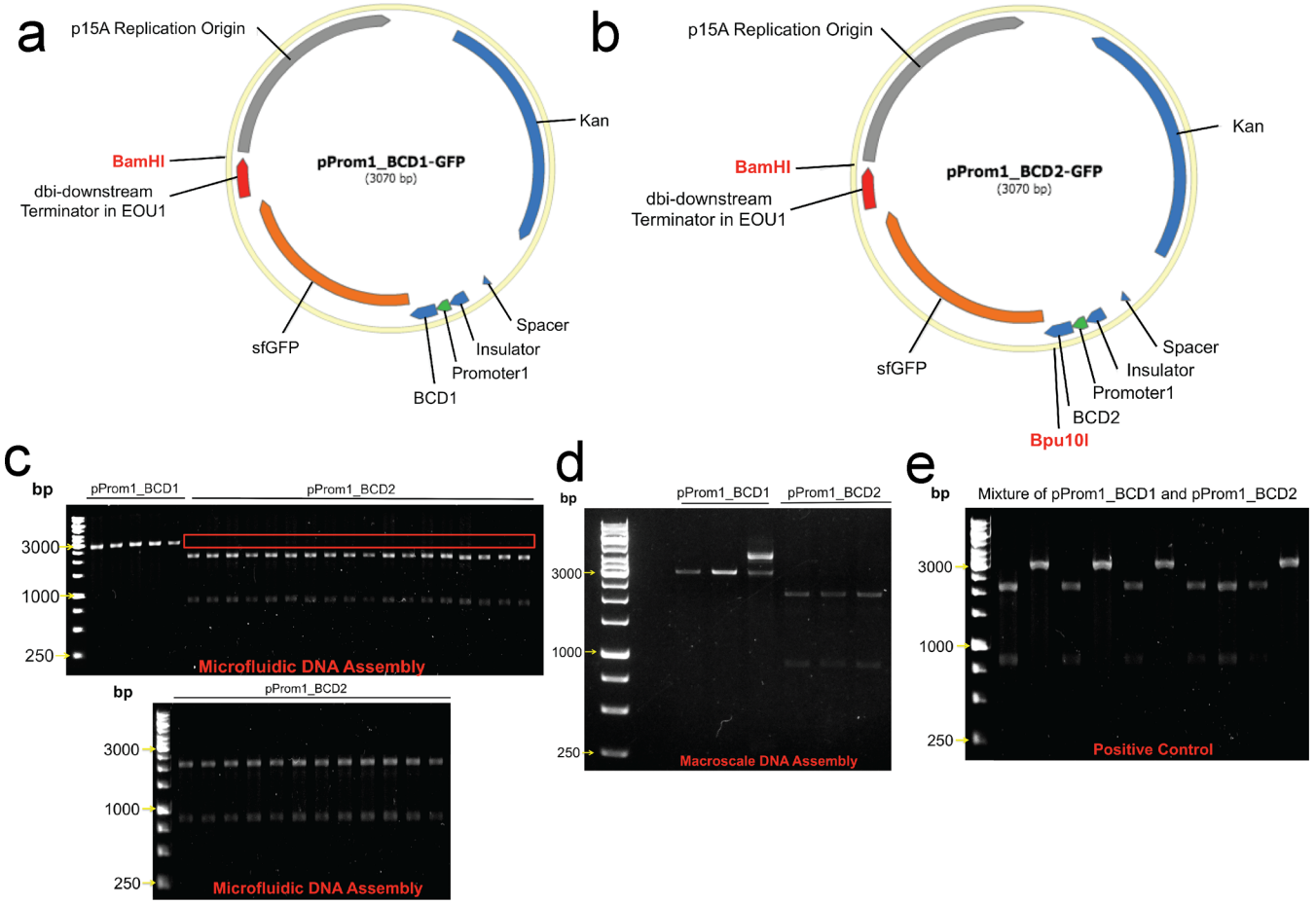

Figure 4. Verification of cross-contamination using hybrid microfluidics. (a) Schematic of plasmid (a) pProm1_BCD1-gfp and (b) pProm1_BCD2-gfp. Both plasmids have a common restriction site, BamHI, whereas only pProm1_BCD2-gfp has a Bpu10I restriction site. After forming these plasmids using microfluidics, 30 colonies were picked from pProm1_BCD2-gfp and digested with both restriction enzymes to verify cross-contamination. Two 1% gel electrophoresis images show the digested plasmids using (c) microfluidics and (d) 0.7 mL tubes. The red box (in c) shows bands in pProm1_BCD1 that are not present in pProm1_BCD2. Fewer colonies were picked for (d) macroscale and (e) positive control experiments since they are used to verify our microfluidic experiments. (e) A 1% gel electrophoresis image showing the results of mixing both plasmids in the same tube followed by digestion (positive control). All gels contained the 1 kb DNA ladder.

with the droplet containing assembled plasmids and non-ligated DNA fragments (Figure 2c). One elastomeric microvalve (labeled as 5; Supporting Information Figure S2) is used to prevent the coalescence of two droplets containing two different assembled plasmids. When the valve is closed, this allows the merging of two droplets, a droplet with cells and a droplet containing the assembled plasmid, without cross-contamination with other droplets in the incubation channel. In addition to the valves, this region also has two fabricated 2.0 × 0.3 mm bare electrodes (with no coated dielectric), which are used to pulse and electroporate the cells. The gap between the two electrodes is 100 μm (Figure 2d).

To demonstrate our newly developed microfluidic automated platform, we experimentally implemented and validated our

DOI: 10.1021/acssynbio.5b00062
ACS Synth. Biol. 2015, 4, 1151−1164

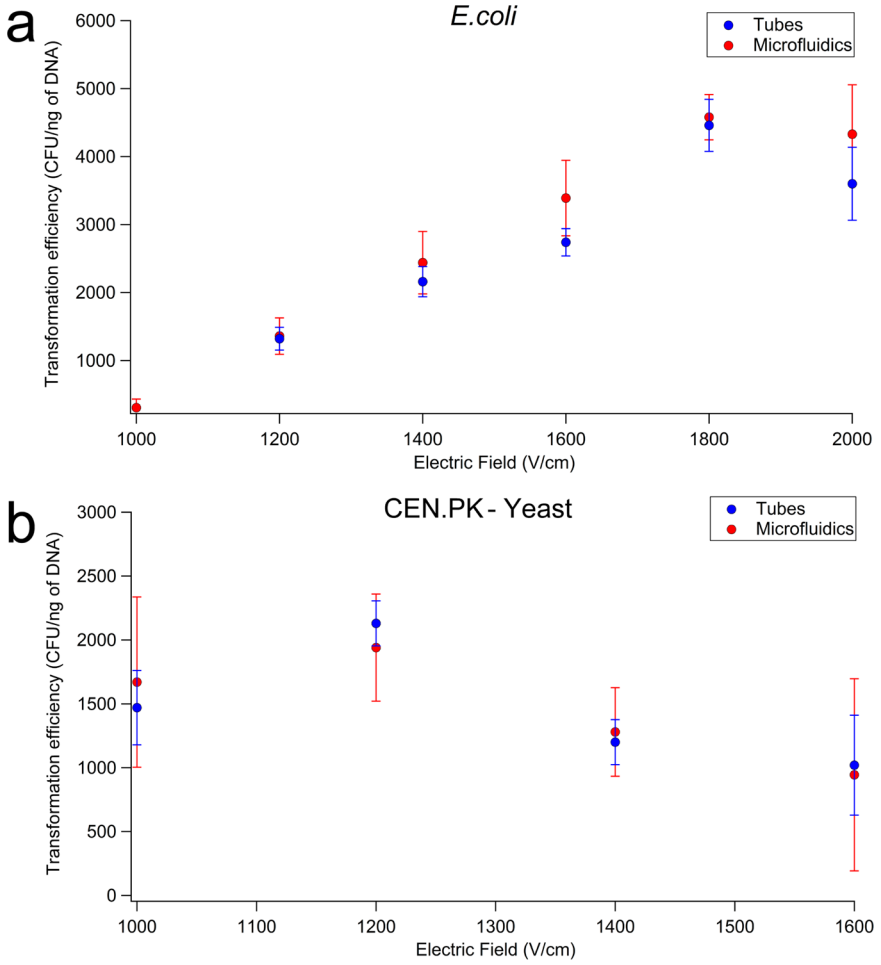

Figure 5. Electroporation optimization. Graphs show transformation efficiency (colony forming units per nanogram of assembled pProm1_BCD1-gfp DNA) as a function of applied electric field in (a) *E. coli* and (b) CEN.PK yeast. Microfluidic results (shown in red) are not significantly different from electroporation experiments conducted in cuvettes (shown in blue). Error bars are ±1 SD for three replicates.

method for Golden Gate, Gibson, and yeast DNA assemblies. We used our device to design two sets of 16 plasmids: one set of plasmids for Golden Gate and Gibson assembly, which contains a p15A origin of replication gene and kanamycin selection marker for bacteria, and one set of plasmids for yeast assembly, which contains both a 2 micron origin of replication gene with a tryptophan selection marker for yeast and an F1 origin of replication gene with an ampicillin selection marker for bacteria. Both sets of plasmids have two common sets of DNA inserts: four promoter (Prom) variants (1, 2, 9, 11) and four bicistronic design (BCD) variants (1, 2, 20, 21) coupled with a *gfp* gene. Prior to DNA assembly, these fragments for each assembly method are digested with DpnI (as well as BsaI for Golden Gate assembly) and gel purified (Figure 3a–c). After purification, vector backbone parts are placed in a vacuum concentrator (Thermo Fisher) for 5–10 min at 65 °C to match the concentrations of the other DNA parts (i.e., BCDs and promoters). To setup 16 DNA assembly reactions, an automation system was designed and programmed to control droplet movement and feedback sensing derived from previous studies and is modified to control external hardware such as control switches, syringe pumps, pressure controller, Peltier heater, and function generator (Supporting Information Figure S3). Although our automation system and device configuration is currently set up for generating 16 DNA assembly reactions, in the future, we propose that additional DNA insertions and combinations will be compatible with these devices with different electrode sizes and configurations.

Cross-Contamination Study. A key advantage with DMF is individual addressability and liquid handling of droplets. This feature allows droplets to serve as discrete microvessels, an important attribute in which reactions can be carried out without cross-talk between samples to reagents. This attribute typically assumes that there are multiple electrode paths (e.g., M × N array of electrodes) for each individual droplet, which eliminates the possibility of cross-contamination between samples. If only one electrode path (or a few paths) is used to drive droplet movement and mixing, then cross-contamination may occur if complex biological solutions are used (e.g., DNA fragments) due to droplet static friction or biofouling on the surfaces of the device. One method presented in literature to avoid cross-contamination is to incorporate additional wash steps in the procedure.[53] This method is appropriate but requires (1) additional reservoirs for the wash solvent and for storing waste droplets and (2) additional droplet movement steps that may further exacerbate cross-contamination on the device. Here, in our study, we applied a different strategy to avoid cross-contamination by adding surfactant additives in our complex biological solutions[54] and a biocompatible oil filler fluid, HFE 7500[55] (as opposed to silicone oil). Since this is the first time that this method has been applied to DNA assembly

DOI: 10.1021/acssynbio.5b00062
ACS Synth. Biol. 2015, 4, 1151–1164

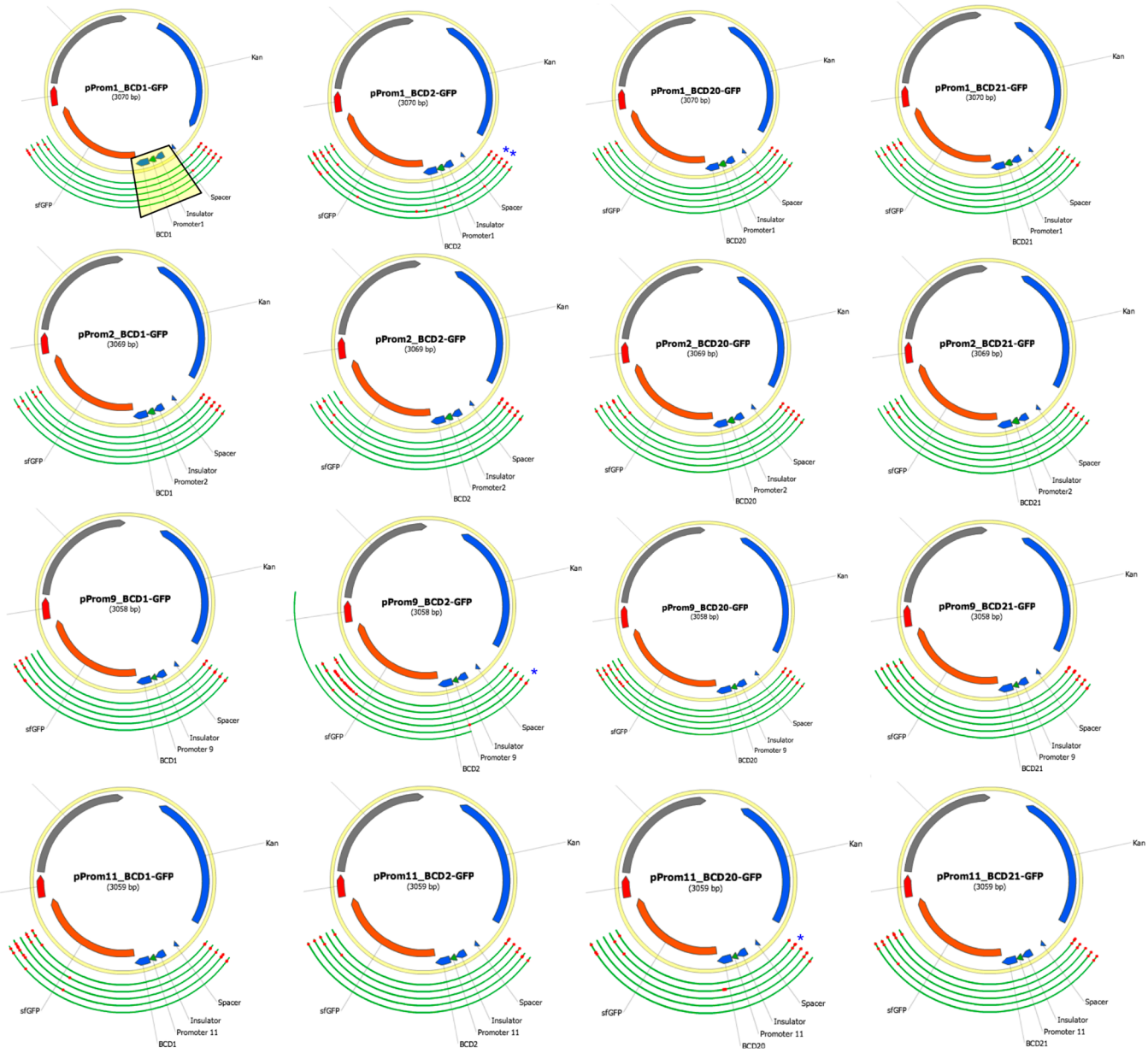

Figure 6. Sequencing results for Golden Gate DNA assembly. A library of 16 DNA plasmids was created using our microfluidic device. Five colonies (that displayed green) were picked from LB agar plates, stored in 10 mM Tris-Cl, pH 8.5, and sequenced. The green portions of the sequencing arcs show regions where the sequencing results matches the expected sequence, and the red portions of the sequencing arcs show regions where the sequencing result does not match the expected sequence.[80] The region spanning the BCD, insulator, promoter (Prom), and neighboring portions of the vector backbone showed a high degree of sequence matching (~95%; highlighted by a yellow box). The blue asterisk beside the sequencing arc represents incorrect clones and is considered to be a failed assembly.

and transformation on hybrid microfluidic devices, we wanted to evaluate cross-contamination on our devices.

To examine if cross-contamination exists between the DNA samples that are generated on-demand, we assembled two plasmids: pProm1_BCD1 (Figure 4a) and pProm1_BCD2 (Figure 4b). Specifically, we assembled pProm1_BCD1 using the protocol described in Methods 15 times using the same electrode path, mixing electrodes, and incubation channel. Next, we assembled a droplet (representing the 16th assembled plasmid) containing pProm1_BCD2 following the same protocol and using the same electrode path, mixing channel, and incubation channel as before. After incubation, these 16 droplets are individually mixed with cells and electroporated and plated for colony growth. Following mini-prep and restriction digestion, cross-contamination is examined by gel electrophoresis (Figure 4c–e). Thirty colonies are picked from the pProm1_BCD1 and pProm1_BCD2 plate and are verified by gel electrophoresis of the digested plasmids. As shown in Figure 4c, every colony from pProm1_BCD1 has one band at ~3 kb (matching the full assembled plasmid), whereas every colony from pProm1_BCD2 has two bands, at ~0.9 and ~2.1 kb, showing that the 30 colonies picked are pProm1_BCD2. From our statistical analysis (see Supporting Information), this is suggestive that cross-contamination is not a problem using our microfluidic device (i.e., with 95% confidence level, cross-contamination is less than 10%). In addition, we conducted this experiment in tubes (Figure 4d), which further confirmed our microfluidic gel profile. Furthermore, as shown in Figure 4e, we

DOI: 10.1021/acssynbio.5b00062
ACS Synth. Biol. 2015, 4, 1151–1164

conducted a positive control in which we mix both BCD1 and BCD2 in the same tube and found a profile that has a random mixture of colonies containing both types of plasmids. This suggests that if contamination is present on our devices then our microfluidic gel profile will give a mixture of bands containing both digested plasmids.

Transformation and Sequencing. Microfluidics is ideally suited to incorporate electroporation due to the relatively low potential needed to generate high electric field strength with microelectrodes and the simplicity of handling and manipulating cells.[56−58] Two gold microelectrodes were patterned on our device to apply a square DC potential to a droplet containing DNA (e.g., pProm1_BCD1 plasmid) and cells (bacteria or yeast). When there is no droplet across these electrodes, the continuous oil phase prevents any electric interaction (i.e., short) between the pair. To activate electroporation, our feedback system (with impedance sensing[59,60]) detects the droplet on the microelectrodes, immediately stops the oil phase flow (replacing the inlet containing cells), and closes the valve near the cell inlet. After this, our automation system will deliver three 100 ms square DC pulses to the droplet containing cells and plasmid (and non-assembled DNA fragments). The oil phase (i.e., HFE 7500) will drive the electroporated droplet into a tube. We varied the field intensity in the range of 1000−2000 V/cm to optimize the intensity that will result in the highest transformation efficiency for our microfluidic setup (Figure 5). As expected, higher electric field intensities yielded higher transformation efficiencies for *Escherichia coli*, where we achieved a maximum efficiency 4.58×10^3 cfu/ng of assembled pProm1_BCD-gfp DNA (110 ± 8 colonies; $N = 3$) at 1800 V/cm (Figure 5a). For CEN.PK yeast, lower fields yielded a maximum efficiency of 1.90×10^3 cfu/ng of DNA (21 ± 6 colonies; $N = 3$) at 1200 V/cm. Higher electric fields saw slight decreases in transformation efficiency, as these higher fields may be killing the cells rather than inserting DNA into the cell. For comparison, we conducted electroporation in cuvettes and found similar values (4.46×10^3 cfu/ng, 137 ± 16 colonies, $N = 3$ in DH5α; and 2.13×10^3 cfu/ng, 32 ± 3 colonies, $N = 3$ in CEN.PK) in transformation efficiency as that with our microfluidic electroporator.

After incubation and electroporation, *E. coli* samples are collected and cultured in tubes for 1 h and plated for colonies. For the highest transformation efficiency, on average, 110 colonies are observed on the plate, where ∼100 (90%) of the colonies displayed a green color (due to the *gfp* gene) and ∼10 (10%) colonies showed a white color (Supporting Information Figure S4). These ratios were similar to the macroscale approach, which yielded, on average, 137 colonies (125 green and 12 white colonies). These white colonies are likely carrying a plasmid without properly assembled DNA inserts (gfp-BCD and promoter) and are possibly due to self-ligation of the vector backbone. For each assembled plasmid (16 total) using Golden Gate and Gibson, we picked five green colonies and sequenced each one, giving us a total of 160 sequenced plasmids (that is, 80 for each assembly method). For yeast assembly, we picked three yeast colonies to mini-prep and to transform in Turbo *E. coli*. Five *E. coli* colonies for each assembled plasmid are screened (green colony color) and sequenced to confirm the completion of the *in vivo* DNA assembly in yeast (that is, the plasmid contained all inserted DNA fragments: BCD-gfp and promoter). Yeast assembly yielded fewer bacterial colonies (∼35 green colonies and 3 white colonies) in Turbo *E. coli* compared to that with Golden Gate and Gibson assemblies. The sequencing results for Golden Gate DNA assembly are shown in Figure 6. Each plasmid map shows five Sanger sequencing results (one arc for each of the five picked clones) spanning the assembled promoter and BCD inserts. The green portions of the sequencing arcs show regions where the sequencing result matches the expected sequence, and the red portions of the sequencing arcs show regions where the sequencing result does not match the expected sequence (e.g., mutations, insertions, deletions). The sequencing results typically indicate putative mutations at the beginning and end of the Sanger sequencing reactions, which is not surprising given that Sanger sequencing quality is low at the beginning and end of a read. Excluding the beginning and end of the Sanger sequencing reactions and regions that are 20 bp upstream or downstream of the overhang/overlap assembly regions in the vector backbone (e.g., in the middle of the *gfp* gene), we obtained a high percentage of perfect sequence clones (76 out 80 = 95%) for the region spanning the BCD, insulator, promoter, and neighboring portions of the vector backbone. We also sequence validated the microfluidic Gibson and yeast assemblies, which showed similar results to those of the microfluidic Golden Gate assemblies. Gibson showed a perfect (80 of 80 = 100%) percentage of correct clones (Supporting Information Figure S5), whereas yeast assembly (70 of 72 = 97.2%) also shows a high percentage of correct clones (Supporting Information Figure S6) for the picked colonies. For yeast assembly, Sanger sequencing reactions failed for two out of the five colonies picked for four of the assembled plasmids (pProm2_BCD1, pProm9_BCD1, pProm11_BCD1, pProm1_BCD2), resulting in fewer sequenced clones. These sequencing results show a high success rate using our microfluidic method for three DNA assembly methods.

Future Outlook. We have engineered a new automated microfluidic device for synthetic biology. Specifically, we assembled two sets of 16 plasmids using three different assembly methods (Golden Gate, Gibson, and TAR cloning) with on-chip incubation, temperature control, and automated electroporation. While microfluidics has been used for DNA assembly[23,61,62] and transformation,[57,58,63] the methods previously described do not integrate three DNA assembly methods with on-chip temperature control and electroporation (that is, either DNA assembly or transformation is conducted off-chip). The new method reported here allows for straightforward, on-demand, and parallel assembly of plasmids, where they are inserted into the cells and are ready to use for plating.

The new method reported here is a hybrid microfluidic format (i.e., integrating different microfluidic paradigms on one platform) and joins a list of several other hybrid microfluidics formats that are used to screen the effects of ionic liquid on single microbe cells[51] and to process samples for chemical separation applications.[50,52] The DMF technique has a key advantage of on-demand liquid handling due to its independent addressability of electrodes and thereby individual droplets. This allows for an ease of mixing multiple reagents on-demand and is an important attribute for integrating various molecular biological processes[53,64,65] on microfluidics. Furthermore, DMF has the potential of scalability and therefore this can enable facile control capabilities to actuate multiple electrodes. Currently, the most commonly fabricated DMF devices are designed with linear tracks of electrodes with individual connections (as shown in this study), but the two-dimensional

DOI: 10.1021/acssynbio.5b00062
ACS Synth. Biol. 2015, 4, 1151−1164

Table 1. Comparison of Microfluidic Platforms for DNA Assembly

parameter	microfluidic platforms for DNA assembly			
	Lin et al.[61]	Liu et al.[62]	Linshiz et al.[23]	this article
type of microfluidics	DMF	DMF	valve-based channel	droplets-in-channel and DMF
dispensing volume	300 nL	300 nL	150 nL	200 nL
total volume of DNA mixture	2.1 μL	2.1 μL	10 μL	0.8 μL (Golden Gate, Gibson) 0.6 μL (Yeast)
DNA assembly method(s)	fast-link DNA ligation	fast-link DNA ligation	Golden Gate, Gibson	Golden Gate, Gibson, yeast assembly
no. of DNA fragment insertions	1	1	2, 4, 8	2
no. of plasmid combinations	4	4	16	16 (2 sets)
heating?	no, room temp.	no, room temp.	yes, entire device	yes, region specific
transformation on-chip?	no	no	no	yes, electroporation

wiring limits the number of electrodes that can be fabricated on a substrate, hence reducing the overall throughput. We propose in the future to increase the throughput (i.e., assembling more than 16 plasmids at a time) on these devices by creating multiple electrodes that can be addressed with fewer connections by replacement of active matrix switching[66,67] or with vertical interconnects that are inherently fabricated on printed circuit boards.[68,69] The DMF technique also has some disadvantages: there is no elegant means of storing and incubating many droplets over hours at a time, as droplets may lead to biofouling the surface of the device or to evaporation over time. However, droplet microfluidics (a technique that manipulates and drives droplets-in-flow) has been shown to be a method to generate and incubate droplets inside their channels or pockets for many hours during an experiment without any biofouling.[70−72] We propose that the different methods presented here are complementary and will be suitable for other biological applications in the future.

We chose four bicistronic (BCD) variants coupled with a *gfp* gene and four promoter variants to be assembled into two vector backbones as a test case for the new microfluidic method because this is a well-suited model for testing DNA assembly protocols.[23] In Linshiz et al.,[23] they have enabled protocol standardization across a couple of laboratory platforms (such as robotics and microfluidics) and validated their new protocol by automating DNA assembly of these plasmid variants using Golden Gate and Gibson methods. Until now, Golden Gate, Gibson, and TAR cloning have never been used to assemble this model plasmid on a hybrid microfluidics platform (Table 1). In fact, this is the first time (to our knowledge) that plasmids have been assembled using low total volumes (<1 μL) with integrated regio-specific temperature control (Supporting Information Figure S7). Using a Peltier heater on a microfluidic device avoids heating the entire device (that is, one area of the device can be heated while another area on the device is at room temperature), and this enables reagents to be stored on the reservoirs (which are maintained at room temperature). This added flexibility is important for reagents like T4 DNA ligase since it may become heat-inactivated at temperatures >50 °C and may lead to biofouling the surface of the device at elevated temperatures. However, with regio-specific temperature heating, droplets containing T4 ligase (or droplets containing similar protein constituents) can be stored at room temperature when they are not used and can be dispensed into subdroplets and driven to the heated region when they are needed for DNA assembly. This also eliminates the requirement of continuously refilling the reservoir with fresh T4 DNA ligase for each assembly reaction and supports continuous automation.

We hypothesized that the combination of digital and droplet microfluidics, which has been used previously for automating droplet mixing and cell culture, might also be useful for automating DNA assembly and cell transformation. The results in Figure 5, Supporting Information Figures S5 and S6, and Figure 6 support this hypothesis, indicating that our technique is capable of assembling and transforming DNA with high efficiencies, an important factor for the *build* and *test* steps in the synthetic biology process. We chose to integrate electroporation with our automated microfluidic device since the automation system (Supporting Information Figure S3) is designed to control the application of electrical pulses to electrodes (for droplet movement) and therefore would be a convenient match for integrating electroporation. Furthermore, to probe the capabilities of our microfluidics technique, we also compared our microfluidics electroporator technique to conventional techniques done in cuvettes. The results in Figure 5 show that our microfluidics technique obtained similar transformation efficiencies (and comparable numbers of transformant colonies) compared to those with electroporation conducted in cuvettes for bacteria and yeast microbes.

The results shown here represent one example of how hybrid microfluidics can be used to automate the synthetic biology process. Other possibilities of using this device (or a derivative thereof) may be useful for future applications in synthetic biology. For example, one can design a device that can be used to assemble multiple plasmids and multiple DNA fragments using a variety of other assembly schemes (e.g., MoClo[73]) or a device to evaluate the functionality of each plasmid by incorporating enzyme screening,[74] creating genetic circuits,[75] or engineering new metabolic pathways.[76] Given the need of automating and expediting the processes of synthetic biology, we propose that this microfluidics method represents a powerful new tool that can be used to assemble plasmids for bioenergy[77] and pharmaceutical[2] applications and beyond.

METHODS

Reagents. Unless otherwise specified, general-use reagents were purchased from Sigma-Aldrich. DH5α electro-competent *E. coli* cells (cat no. C2989K) and Turbo competent *E. coli* (high efficiency) (cat no. C2984H) were purchased from New England Biolabs (Ipswich, MA). CEN.PK yeast strain (which has a TRP deletion) and plasmids/strains used for DNA assembly (see Table S1 for names and part ID nos.) were obtained from the public registry at the Joint BioEnergy Institute (https://public-registry.jbei.org/login). Mini-prep kits were purchased from Qiagen (used for *E. coli*) and Zymo Research (used for CEN.PK).

Microfluidic device fabrication reagents and supplies included SU-8-5, SU-8-2075, S-1811, and SU-8 Developer from

DOI: 10.1021/acssynbio.5b00062
ACS Synth. Biol. 2015, 4, 1151−1164

Microchem (Newton, MA), gold- and chromium-coated glass slides from Telic (Valencia, CA), indium tin oxide (ITO)-coated glass slides (Delta Technologies, Stillwater, MN), Aquapel from TCP Global (San Diego, CA), MF-321 positive photoresist developer from Rohm and Haas (Marlborough, MA), standard KI/I_2 gold etchant from Sigma, CR-4 chromium etchant from OM Group (Cleveland, OH), and AZ-300T photoresist stripper from AZ Electronic Materials (Somerville, NJ). PDMS reagents (Sylgard 184) were purchased from Dow Corning (Midland, MI).

DNA Fragment Preparation: Golden Gate Assembly. *PCR Amplification.* Plasmids pFAB4876, pFAB4884, pFAB4924, and pFAB4932, were extracted from *E. coli* using spin miniprep kits (Qiagen; Valencia, CA) and served as DNA templates for the PCR amplification of promoter fragments Promoter1, Promoter2, Promoter9, and Promoter11, respectively. Similarly, pFAB4876, pFAB4877, pFAB4882, and pFAB4883 also served as DNA templates for the PCR amplification of the four BCD variant fragments BCD1_gfp, BCD2_gfp, BCD20_gfp, and BCD21_gfp, respectively. Plasmid pFAB4876 served as the DNA template for the PCR amplification of the vector backbone. Primers MS_02148_(Backbone_p4001)_forward and MS_02149_(Backbone_p4001)_reverse were used for the amplification of the vector backbone; primers MS_02150_(P1)_forward and MS_02151_(P1)_reverse, MS_02154_(P2)_forward and MS_02155_(P2)_reverse, MS_02154_(P2)_forward and MS_02160_(P9)_reverse, and MS_02154_(P2)_forward and MS_02161_(P11)_reverse were used for the amplification of fragments Promoter1, Promoter2, Promoter9, and Promoter11, respectively; primers MS_02152_(BCD1-GFP)_forward and MS_02153_(BCD1-GFP)_reverse were used for the amplification of the four BCD variant fragments (see Supporting Information Table S2 for primer sequences). Fifty microliter PCR reactions consisted of 2.5 μL (2.5 μM) of each forward and reverse primer, 1 μL of template, 1 μL of dNTPs (10 mM), 0.5 μL of high-fidelity iProof phusion polymerase (BioRad; Hercules, CA), 10 μL of high-fidelity phusion buffer, and 32.5 μL of deionized water. Four 50 μL PCR reactions (200 μL total) were performed for each fragment amplified. The following PCR thermocycling conditions were used: denaturation at 98 °C for 30 s, 38 cycles of denaturation at 98 °C for 20 s, annealing at 68 °C for 30 s, and elongation at 72 °C for 15 s for each kilobase, with a final extension at 72 °C for 10 min.

DpnI and BsaI Digest and Purification. Following PCR amplification, the residual (methylated) DNA template in each PCR reaction was DpnI digested at 37 °C for 1 h. Each 110 μL digest reaction consisted of 95 μL of PCR product, 11 μL of 10× FastDigest buffer, 1.5 μL of FastDigest DpnI (Thermo Fisher Scientific; Waltham, MA), and 2.5 μL of deionized water. DpnI was inactivated at 80 °C for 5 min, and DNA purification of each DpnI reaction was conducted with a PCR purification kit (Qiagen) according to the manufacturer's protocol, with each purified sample eluted with 50 μL of elution buffer.

Following DpnI digest and purification, 70 μL digestion reactions consisting of 50 μL of purified DpnI reaction, 7 μL of NEB4 buffer, 0.7 μL of BSA, 5 μL of BsaI, and 7.3 μL of deionized water were performed overnight at 37 °C. BsaI was deactivated at 65 °C for 20 min. Digested samples were run on a 0.8% agarose gel followed by gel purification (Qiagen) according to manufacturer's protocol. The DNA concentrations of the purified DNA fragments were measured using a NanoDrop (Thermo Fischer Scientific).

DNA Fragment Preparation: Gibson Assembly. *PCR Amplification.* Plasmid pFAB4876 served as the DNA template for the PCR amplification of the vector backbone using primer pair DVA00220_(vector_BB)_forward and DVA00221_(vector_BB)_reverse (Integrated DNA Technologies, IDT; Coralville, IA). Plasmids pFAB4876, pFAB4884, pFAB4924, and pFAB4932 served as the DNA templates for the PCR amplification of promoter fragments Promoter1, Promoter2, Promter9, and Promoter11, respectively, using primer pairs DVA00222_(Prom1)_forward and DVA00223_(Prom1)_reverse, DVA00222_(Prom1)_forward and DVA00226_(Prom2)_reverse, DVA00222_(Prom1)_forward and DVA00227_(Prom9)_reverse, and DVA00222_(Prom1)_forward and DVA00228_(Prom11)_reverse, respectively. Similarly, pFAB4876, pFAB4877, pFAB4882, and pFAB4883 also served as DNA templates for the PCR amplification of the four BCD variant fragments BCD1_gfp, BCD2_gfp, BCD20_gfp, and BCD21_gfp, respectively. Primers DVA00224_(BCD1)_forward and DVA00225_(BCD1)_reverse were used for the amplification of the four BCD variant fragments. Fifty microliter PCR reactions consisted of 5 μL (5 μM) of each forward and reverse primer, 10 μL of template (5 ng/μL), 25 μL of 2× hot start high-fidelity Q5 PCR master mix (NEB), and 5 μL of deionized water. The following PCR thermocycling conditions were used: denaturation at 98 °C for 30 s, 35 cycles of denaturation at 98 °C for 20 s, annealing at different temperatures ranging from 62.9 to 67.2 °C for 20 s, and elongation at 72 °C for 20 s for each kilobase, with a final extension at 72 °C for 10 min.

DpnI Digest and Purification. Following PCR amplification, residual (methylated) DNA template in each PCR reaction was DpnI digested at 37 °C for 1 h. Each 60 μL digest reaction consisted of 50 μL of PCR product, 6 μL of 10× FastDigest buffer, 1 μL of FastDigest DpnI (Thermo Fisher Scientific), and 3 μL of deionized water. DpnI was inactivated at 80 °C for 5 min, and the digested samples were run on a 1.0% agarose gel followed by gel purification (Qiagen kit no. 28704) of the desired DNA bands, according to the manufacturer's protocol. The DNA concentrations of the purified DNA fragments were measured using a NanoDrop (Thermo Fischer Scientific).

DNA Fragment Preparation: Yeast Assembly. *PCR Amplification.* Plasmids pFAB4876, pFAB4884, pFAB4924, and pFAB4932 served as the DNA templates for the PCR amplification of promoter fragments Promoter1, Promoter2, Promter9, and Promoter11, respectively. Primer pairs DVA00323_(Prom1)_forward and DVA00324_(Prom1)_reverse, DVA00323_(Prom1)_forward and DVA00326_(Prom2)_reverse, DVA00323_(Prom1)_forward and DVA00327_(Prom9)_reverse, and DVA00323_(Prom1)_forward and DVA00328_(Prom11)_reverse, respectively, were used for the amplification of Promoter1, Promoter2, Promoter9, and Promoter11. Similarly, pFAB4876, pFAB4877, pFAB4882, and pFAB4883 also served as DNA templates for the PCR amplification of the four BCD variant fragments BCD1_gfp, BCD2_gfp, BCD20_gfp, and BCD21_gfp, respectively. Primers DVA00224_(BCD1)_forward and DVA00325_(BCD1)_reverse were used for the amplification of the four BCD variant fragments. Plasmid pRS424 from *E. coli* served as the DNA template for the PCR amplification of the vector backbone. Primers DVA00321_(vector_Bb)_forward and DVA00322_(vector_Bb)_reverse

DOI: 10.1021/acssynbio.5b00062
ACS Synth. Biol. 2015, 4, 1151−1164

were used for the amplification of the vector backbone. Fifty microliter PCR reactions consisted of 5 μL (5 μM) of each forward and reverse primer (see Table S2 for primer sequences), 10 μL of template (5 ng/μL), 25 μL of 2× hot start high-fidelity Q5 PCR master mix (NEB), and 5 μL of deionized water. The following PCR thermocycling conditions were used: denaturation at 98 °C for 30 s, 35 cycles of denaturation at 98 °C for 20 s, annealing at different temperatures ranging from 62.9 to 71.4 °C for 20 s, and elongation at 72 °C for 20 s for each kilobase, with a final extension at 72 °C for 10 min.

DpnI Digest and Purification. Following PCR amplification, residual (methylated) DNA template in each PCR reaction was DpnI digested at 37 °C for 1 h. Each 60 μL digest reaction consisted of 50 μL of PCR product, 6 μL of 10× FastDigest buffer, 1 μL of FastDigest DpnI (Thermo Fisher Scientific), and 3 μL of deionized water. DpnI was inactivated at 80 °C for 5 min, and the digested samples were run on a 1.0% agarose gel followed by gel purification of the desired DNA bands, according to the manufacturer's protocol. The DNA concentrations of the purified DNA fragments were measured using a NanoDrop.

Microfluidic Device Fabrication. Microfluidic devices were fabricated in the University of California Biomolecular Nanotechnology Center (UC Berkeley−BNC) fabrication facility, using a transparent photomask printed at CAD/Art Services Inc. (Bandon, OR). Digital microfluidic device bottom plates bearing patterned electrodes and contact pads were formed by photolithography and etching as described previously. Briefly, devices with S1811 photoresist (from Telic) were exposed to UV for 5 s (40 mW cm^{-2}) using an OAI Series 200 Aligner (San Jose, CA) and were developed by immersing in MF-321 for ∼2 min and rinsed with deionized water (diH_2O). Gold was etched by immersing in gold etchant (∼2 min), which was followed by chromium etchant by immersing in CR-4 (∼10 s). These devices were then rinsed with diH_2O, immersed in AZ 300T (5 min) to remove remaining photoresist, and washed in DI water. To prepare for dielectric coating, these devices were immersed in acetone (2 min), isopropanol (2 min), and water (1 min) and dried with N_2. They were then placed on a hot plate (120 °C, 10 min) for postbaking. The devices were plasma-treated under 20% O_2 and RF power of 20 W for 3 min and were then coated with a 7 μm layer dielectric using SU-8-5 following Microchem's instructions for spin speed and bake times. For the channel fluidic layer and spacer features, the devices were then plasma-treated (using the same conditions as above) and coated with a layer of SU-8-2075 to pattern channels and a spacer with a height of 140 μm. Spin speeds, soft and hard bake times, and development times followed Microchem's instructions. After development, these were rinsed, dried with isopropanol and diH_2O, and hard-baked for 15 min at 200 °C. For a hydrophobic layer, the DMF devices and ITO top plates were coated with 0.2 μm filtered Aquapel. After 15 min, the Aquapel was removed with a Kimwipe and rinsed with diH_2O. This was then dried with N_2 and left at room temperature for 1 h.

The valve layer on the digital microfluidic device was constructed using soft lithography method. The control layer is composed of a 100 μm deep channel for pneumatic valve actuation using a VSO-EP Parker miniature pressure controller (orifice size 0.01″, pressure range 0−15 psi, internal vent; Precision Fluidics, Hollis, NH). The control layer master was made of a negative photoresist SU-8-2075 following photolithography methods. The master was silanized with trichloro-(1*H*,1*H*,2*H*,2*H*-perfluorooctyl) silane (97%, Aldrich) overnight. PDMS consisting of monomer and curing agent (10:1 ratio) was poured onto the control layer, degassed overnight, and baked at 85 °C for 30 min. The PDMS was then peeled, and access holes were punched using a 1.25 mm puncher (World Precision Instruments, Sarasota, FL). The fluidic and the control layers were separated by a thin PDMS membrane, which was created by spinning PDMS onto a 4″ silicon wafer at 500 rpm (acceleration: 100 rpm) for 10 s and then 1000 rpm (acceleration: 300 rpm) for 30 s to generate a ∼100 μm thick membrane. After partially curing for 5 min at 80 °C, the control layer (∼5 mm thick) and the thin membrane (with the wafer) were plasma-treated (Harrick Plasma, Ithaca, NY), bonded, and then placed on the hot plate at 80 °C for 10 min for complete curing. The control layer and the thin PDMS membrane were peeled off from the wafer. After peeling, inlet and outlet holes were punched using a 0.5 mm puncher and then placed in the oxygen plasma for 3 min. The digital microfluidic device that contains the SU-8 fluidic layer was placed in a vacuum chamber with 3-aminopropyltrimethoxysilane for 12 h. The amino groups attached onto the PDMS surface, which can react with the epoxy groups on the SU-8 surface through an amine-epoxide reaction.[78] After bonding, the device is placed on the hot plate at 80 °C for 1 h to strengthen the bond between the PDMS and SU-8.

Microfluidic DNA Assembly and Transformation. Driving potential (∼100−120 V rms) were generated by amplifying the sine wave output of a function generator (Agilent Technologies, Santa Clara, CA) operating at 8 kHz. The application of the driving potentials was managed using an automated feedback control system[47,59,60,79] using a circuit described elsewhere.[59,60] Briefly, to describe the automated feedback control system, the droplet position is sensed as a function of the measured potential, V_{sense}. When V_{sense} is measured across an electrode not bearing a droplet, V_{sense} is ∼0.05 V because oil has no or very little polarizability and therefore has very high impedance, >∼10 GΩ. However, when V_{sense} is measured across an electrode bearing a liquid droplet, the impedance reduces to ∼0.1−10 MΩ, which causes V_{sense} to increase beyond 0.05 V (see below for the description of V_{thres}). To move a droplet onto a given destination electrode on the bottom plate, a 200 ms pulse of driving potential is applied to the destination electrode relative to the top-plate ITO electrode. During the last 10 ms of the voltage pulse, the potentiometer is triggered to deliver 5% of the voltage to the positive terminal of the buffered op-amp (MCP6004, Microchip, Brampton, ON, Canada), the output of which is connected to the analog input of an RBBB Arduino microcontroller (Modern Device, Providence, RI). The magnitude of the output voltage (hereafter, V_{sense}) is proportional to the droplet volume between the destination electrode on the bottom plate and the top plate electrode (see Supporting Information Figure S8). Threshold values were recorded for the liquids used here (V_{thres} ∼ 0.15 V for ∼0.2 μL volume). After each voltage pulse, the software compares the measured impedance to the threshold value, and if the measured impedance is below the threshold, then additional voltage pulses are triggered with +5 V higher magnitudes until the droplet completes the desired operation. If droplets are being dispensed, then the measured impedance is compared to the threshold and the dispensing process is repeated if V_{sense} is

DOI: 10.1021/acssynbio.5b00062
ACS Synth. Biol. 2015, 4, 1151−1164

not within ±1% of V_{thres}. See Supporting Information Figure S3 for connectivity of the automation system.

To start the DNA assembly process, 1 mL of HFE 7500 (i.e., oil) was pipetted onto the digital microfluidic (DMF) surface. Next, 1.5 μL droplets containing gel-extracted BCD-gfp (30−40 ng/μL), promoter DNA fragments (30−40 ng/μL), and vector backbone (30−40 ng/μL) were pipetted onto reservoirs while simultaneously applying a driving potential to the reservoir electrodes to maintain fluid on the reservoir. For Golden Gate DNA assembly, an additional 1.5 μL of T4 DNA ligase (2.5 U/μL) with a 0.05% w/v F-127 Pluronic droplet was also pipetted onto a reservoir, whereas for Gibson assembly, a droplet of 2× Gibson assembly master mix with 0.05% w/v F-127 Pluronic was pipetted. For yeast assembly, no additional droplets were required for assembly. An indium−tin oxide (ITO)-coated glass was placed on top of the device and connected to the feedback sensing circuit. Once assembled, ∼0.2 μL of a droplet containing BCD-gfp, promoter, and vector backbone was actively dispensed and actuated to the mixing region on the device. To refill reservoirs, a capillary was attached to the edge of the reservoir via a fabricated SU-8 channel and fluid was pressure driven into the reservoir (see Shih et al.[51] for more details). For Golden Gate DNA assembly, ∼0.2 μL of T4 DNA ligase was actively dispensed and combined with the mixture described above. For Gibson DNA assembly, ∼0.2 μL of 2× Gibson assembly master mix was dispensed and mixed. These four droplets (for Golden Gate and Gibson) were combined and mixed in a circular fashion (2 to 3 times) on the electrodes near the digital-to-droplet interface. For yeast assembly, three droplets containing BCD-gfp, promoter DNA fragments, and vector backbone were mixed and circulated.

After droplet operations on the DMF device, neMESYS syringe pumps (Cetoni, Korbussen, Germany) and miniature pneumatic actuators (Parker) were activated to transfer the droplet into the channel area for incubation and electroporation. As shown in Figure S2a−f, droplets created by DMF were suctioned into the channel area by pulling air using the syringe pump at a flow rate of 0.1 μL/s. During this time, the impedance system applies a 100 ms, 100 V signal with a 50 ms step to determine if the droplet is on the electrode. Once there was no droplet detected on the electrode (as measured by impedance), the syringe-vacuum stops and the oil phase flow (i.e., HFE 7500) at a flow rate of 5 μL/s was activated, with valves opening (shown in white) and closing (shown in black) to maintain pressure of the oil phase flow. This DNA assembly process was repeated 15 times to generate a total of 16 plasmid combinations. In the incubation channel, the droplets were incubated for 10 min for Golden Gate and yeast assemblies (at room temperature) and 15 min for Gibson assembly (at 50 °C). For Gibson assembly, the Peltier heater is activated by the Arduino RBBB and was immediately ramped to the desired temperature after suctioning the last droplet into the channel (Supporting Information Figure S7 shows the 50 °C region-specific temperature zone).

To insert the DNA plasmid into the microbes, cells in electroporation media (1.0 M sorbitol for yeast and 8 mM Na_2HPO_4, 2 mM KH_2PO_4, and 250 mM sucrose, pH 7.4, for bacteria) were driven from the syringe into the channel using a flow rate of 0.05 μL/s. A droplet of cells was dispensed by applying potential to the electrodes (near the cell inlet) while applying a reverse-flow using the syringe pump at a flow rate of 0.1 μL/s. This droplet of cells was mixed with the plasmid DNA and driven to the electroporation electrodes. Two DC 200 ms pulses of 1800 V/cm (for bacteria) and 1200 V/cm (for yeast) were applied to the mixed droplet containing DNA and cells. After electroporation, the droplet was driven to the outlet by replacing the inlet containing cells with an oil phase (with all valves closed; see Supporting Information Figure S2). The droplet was collected in a tube containing 200 μL recovery media: LB broth for bacteria and deionized water for yeast.

Macroscale DNA Assembly and Transformation. DNA assembly ligation reactions consisted of mixing 1 μL of each DNA fragment (30−40 ng/μL) with 1 μL of the vector backbone (30−40 ng/μL) in microfuge tubes. Each of the 16 combinatorial reactions was incubated for 10 min using Golden Gate assembly (at room temperature), 20 min using Gibson assembly (at 50 °C), and 5 min using yeast assembly (at room temperature). After incubation, 1 μL of the DNA mixture was added to 20 μL of electrocompetent *E. coli* cells for Golden Gate and Gibson assemblies or to 40 μL of electrocompetent CEN.PK cells for yeast assembly (see Supporting Information for preparation of electrocompetent yeast cells). The mixture containing cells and DNA was transferred to 1 mm cuvettes (for *E. coli*) or 2 mm cuvettes (for yeast) and pulsed using a Gene Pulser Xcell electroporation system (BioRad Laboratories Inc.; Pleasanton, CA) using preset protocol parameters for *E. coli* and *S. cerevisiae*. Two-hundred microliters of recovery media (LB media for bacteria and deionized water for yeast) was added to the electroporated mixture. The transformed culture was plated on LB agar with kanamycin (50 μg/mL) (bacteria) or CSM-agar ΔTRP (yeast) plates, and plates were incubated overnight at 37 °C or for 2 days at 30 °C, respectively.

Colony Picking and Sequencing. *Golden Gate and Gibson Assemblies.* Five colonies from each LB agar plate were chosen and grown overnight in LB media with kanamycin. DNA was extracted from the cells by conducting a mini-prep (Qiagen) following the manufacturer's instructions. DNA concentrations were measured by a NanoDrop spectrophotometer (Thermo). DNA samples were submitted for sequencing (QuintaraBio, Albany, CA) with primers (QB3284_fwd and QB3810_rev) shown in Supporting Information Table S3.

Yeast Assembly. Electroporated yeast samples from our microfluidic device were grown overnight in CSM ΔTRP selective media, and five colonies from each plate were chosen. To extract the DNA, we used the Zyppy plasmid miniprep kit (Zymo Research, Irvine, CA; cat no. D4020). We pelleted 5 mL of the yeast culture, resuspended the pellet in 600 μL, and added 100 μL of lysis buffer. We added 1 volume of 0.5 mm zirconia/silica beads (Biospec Products Inc., Bartlesville, OK; cat no. 11079105Z) and placed the tube in a Tissuelyser (Qiagen) for 2 min using a frequency of 30 Hz. The supernatant was then mixed with 350 μL of neutralization buffer in a tube and spun in a microcentrifuge for 5 min at 15 000 rpm. The supernatant was applied to the column and spun for 1 min at 15 000 rpm. Next, 200 μL of Endo wash buffer was applied to the column, the column was spun for 1 min, 400 μL of wash buffer was applied to the column, and it was spun for another minute. The column was then dried on a heating block (∼60 °C) for 10 min, and 30 μL of heated diH_2O (∼60 °C) was added to the column, which was then spun for 2 min at 15 000 rpm. The DNA concentration was measured using the NanoDrop, which typically ranged from 10 to 20 ng/μL.

DOI: 10.1021/acssynbio.5b00062
ACS Synth. Biol. 2015, 4, 1151−1164

After DNA extraction from yeast, the DNA was mixed with 20 μL of Turbo *E. coli* chemically competent cells. The heat shock transformation followed the manufacturer's instructions. The transformed culture (~200 μL) was plated on LB agar supplemented with 50 μg/mL carbenicillin and incubated at 37 °C overnight. Culture tubes containing 5 mL of LB media supplemented with 50 μg/mL carbenicillin were inoculated with transformants (one picked colony per tube) and placed at 37 °C at 200 rpm on a shaker for 4 h. The DNA from these cultures were extracted using a mini-prep kit (Qiagen) following the manufacturer's instructions, and the concentrations were measured using the NanoDrop (ranging from 40 to 50 ng/μL). These DNA samples were sent for sequencing (Genewiz Inc., Berkeley, CA) using primers yeast_fwd and yeast_rev (shown in Supporting Information Table S3).

■ ASSOCIATED CONTENT

Supporting Information

Strains, plasmids, and primers for PCR and sequencing are presented in Tables S1 and S2; a detailed protocol to prepare electrocompetent yeast cells and statistical analysis for cross-contamination is also given. The Supporting Information is available free of charge on the ACS Publications website at DOI: 10.1021/acssynbio.5b00062.

■ AUTHOR INFORMATION

Corresponding Authors

*(S.C.C.S.) Tel.: (510) 928-1245. E-mail: ccshih@lbl.gov.
*(A.K.S.) Tel.: (925) 294-1280. E-mail: aksingh@sandia.gov.

Present Address

#(N.K.) Department of Systems and Synthetic Microbiology, Max Planck Institute for Terrestrial Microbiology & LOEWE Research Center for Synthetic Microbiology (SYNMIKRO), Karl-von-Frisch Strasse 16, D-35043 Marburg, Germany.

Notes

The authors declare no competing financial interest.

■ ACKNOWLEDGMENTS

The authors thank Amanda Reider Apel and Charles Denby for helpul hints with yeast transformation methods, Anna Lechner for quick yeast transformation protocols, Hector Martin Garcia for help with statistical analysis, and Hector Plahar for transferring plasmid and strain files to the JBEI's public registry. This work conducted by the Joint BioEnergy Institute was supported by the U.S. Department of Energy, Office of Science, Office of Biological and Environmental Research, through contract DE-AC02-05CH11231 between Lawrence Berkeley National Laboratory and the U.S. Department of Energy.

■ REFERENCES

(1) Lu, T. K., and Collins, J. J. (2007) Dispersing biofilms with engineered enzymatic bacteriophage. *Proc. Natl. Acad. Sci. U.S.A. 104*, 11197−11202.

(2) Lu, T. K., and Collins, J. J. (2009) Engineered bacteriophage targeting gene networks as adjuvants for antibiotic therapy. *Proc. Natl. Acad. Sci. U.S.A. 106*, 4629−4634.

(3) Westfall, P. J., and Gardner, T. S. (2011) Industrial fermentation of renewable diesel fuels. *Curr. Opin. Biotechnol. 22*, 344−350.

(4) Ro, D. K., Paradise, E. M., Ouellet, M., Fisher, K. J., Newman, K. L., Ndungu, J. M., Ho, K. A., Eachus, R. A., Ham, T. S., Kirby, J., Chang, M. C., Withers, S. T., Shiba, Y., Sarpong, R., and Keasling, J. D. (2006) Production of the antimalarial drug precursor artemisinic acid in engineered yeast. *Nature 440*, 940−943.

(5) Peralta-Yahya, P. P., and Keasling, J. D. (2010) Advanced biofuel production in microbes. *Biotechnol. J. 5*, 147−162.

(6) Huang, H., and Densmore, D. (2014) Integration of microfluidics into the synthetic biology design flow. *Lab Chip 14*, 3459−3474.

(7) Linshiz, G., Goldberg, A., Konry, T., and Hillson, N. J. (2012) The fusion of biology, computer science, and engineering towards efficient and successful synthetic biology. *Perspect. Biol. Med. 55*, 503−520.

(8) Xia, B., Bhatia, S., Bubenheim, B., Dadgar, M., Densmore, D., and Anderson, J. C. (2011) Developer's and user's guide to Clotho v2.0 A software platform for the creation of synthetic biological systems. *Methods Enzymol. 498*, 97−135.

(9) Hillson, N. J., Rosengarten, R. D., and Keasling, J. D. (2012) j5 DNA assembly design automation software. *ACS Synth. Biol. 1*, 14−21.

(10) Cai, Y., Wilson, M. L., and Peccoud, J. (2010) GenoCAD for iGEM: a grammatical approach to the design of standard-compliant constructs. *Nucleic Acids Res. 38*, 2637−2644.

(11) Beal, J., Lu, T., and Weiss, R. (2011) Automatic compilation from high-level biologically-oriented programming language to genetic regulatory networks. *PLoS One 6*, e22490.

(12) Pedersen, M., and Phillips, A. (2009) Towards programming languages for genetic engineering of living cells. *J. R. Soc., Interface 6*, S437−S450.

(13) Bilitchenko, L., Liu, A., Cheung, S., Weeding, E., Xia, B., Leguia, M., Anderson, J. C., and Densmore, D. (2011) Eugene—a domain specific language for specifying and constraining synthetic biological parts, devices, and systems. *PLoS One 6*, e18882.

(14) Galdzicki, M., Clancy, K. P., Oberortner, E., Pocock, M., Quinn, J. Y., Rodriguez, C. A., Roehner, N., Wilson, M. L., Adam, L., Anderson, J. C., Bartley, B. A., Beal, J., Chandran, D., Chen, J., Densmore, D., Endy, D., Grunberg, R., Hallinan, J., Hillson, N. J., Johnson, J. D., Kuchinsky, A., Lux, M., Misirli, G., Peccoud, J., Plahar, H. A., Sirin, E., Stan, G. B., Villalobos, A., Wipat, A., Gennari, J. H., Myers, C. J., and Sauro, H. M. (2014) The Synthetic Biology Open Language (SBOL) provides a community standard for communicating designs in synthetic biology. *Nat. Biotechnol. 32*, 545−550.

(15) Appleton, E., Tao, J., Haddock, T., and Densmore, D. (2014) Interactive assembly algorithms for molecular cloning. *Nat. Methods 11*, 657−662.

(16) Richardson, S. M., Nunley, P. W., Yarrington, R. M., Boeke, J. D., and Bader, J. S. (2010) GeneDesign 3.0 is an updated synthetic biology toolkit. *Nucleic Acids Res. 38*, 2603−2606.

(17) Salis, H. M. (2011) The ribosome binding site calculator. *Methods Enzymol. 498*, 19−42.

(18) Chen, J., Densmore, D., Ham, T. S., Keasling, J. D., and Hillson, N. J. (2012) DeviceEditor visual biological CAD canvas. *J. Biol. Eng. 6*, 1.

(19) Cox, R. S., III, Nishikata, K., Shimoyama, S., Yoshida, Y., Matsui, M., Makita, Y., and Toyoda, T. (2013) PromoterCAD: data-driven design of plant regulatory DNA. *Nucleic Acids Res. 41*, W569−574.

(20) Stevens, J. T., and Myers, C. J. (2013) Dynamic modeling of cellular populations within iBioSim. *ACS Synth. Biol. 2*, 223−229.

(21) Carbonell, P., Parutto, P., Herisson, J., Pandit, S. B., and Faulon, J. L. (2014) XTMS: pathway design in an eXTended metabolic space. *Nucleic Acids Res. 42*, W389−394.

(22) Soh, K. C., and Hatzimanikatis, V. (2010) DREAMS of metabolism. *Trends Biotechnol. 28*, 501−508.

(23) Linshiz, G., Stawski, N., Goyal, G., Bi, C., Poust, S., Sharma, M., Mutalik, V., Keasling, J. D., and Hillson, N. J. (2014) PR-PR: cross-platform laboratory automation system. *ACS Synth. Biol. 3*, 515−524.

(24) Takahashi, C. N., Miller, A. W., Ekness, F., Dunham, M. J., and Klavins, E. (2015) A low cost, customizable turbidostat for use in synthetic circuit characterization. *ACS Synth. Biol. 4*, 32−38.

(25) Linshiz, G., Stawski, N., Poust, S., Bi, C., Keasling, J. D., and Hillson, N. J. (2013) PaR-PaR laboratory automation platform. *ACS Synth. Biol. 2*, 216−222.

DOI: 10.1021/acssynbio.5b00062
ACS Synth. Biol. 2015, 4, 1151−1164

(26) Yordanov, B., Dalchau, N., Grant, P. K., Pedersen, M., Emmott, S., Haseloff, J., and Phillips, A. (2014) A computational method for automated characterization of genetic components. *ACS Synth. Biol. 3*, 578−588.
(27) Gibson, D. G., Young, L., Chuang, R. Y., Venter, J. C., Hutchison, C. A., III, and Smith, H. O. (2009) Enzymatic assembly of DNA molecules up to several hundred kilobases. *Nat. Methods 6*, 343−345.
(28) Engler, C., Gruetzner, R., Kandzia, R., and Marillonnet, S. (2009) Golden Gate shuffling: a one-pot DNA shuffling method based on type IIs restriction enzymes. *PLoS One 4*, e5553.
(29) Engler, C., Kandzia, R., and Marillonnet, S. (2008) A one pot, one step, precision cloning method with high throughput capability. *PLoS One 3*, e3647.
(30) Gibson, D. G., Benders, G. A., Axelrod, K. C., Zaveri, J., Algire, M. A., Moodie, M., Montague, M. G., Venter, J. C., Smith, H. O., and Hutchison, C. A., III (2008) One-step assembly in yeast of 25 overlapping DNA fragments to form a complete synthetic Mycoplasma genitalium genome. *Proc. Natl. Acad. Sci. U.S.A. 105*, 20404−20409.
(31) Shao, Z., Zhao, H., and Zhao, H. (2009) DNA assembler, an in vivo genetic method for rapid construction of biochemical pathways. *Nucleic Acids Res. 37*, e16.
(32) de Jong, H., Ranquet, C., Ropers, D., Pinel, C., and Geiselmann, J. (2010) Experimental and computational validation of models of fluorescent and luminescent reporter genes in bacteria. *BMC Syst. Biol. 4*, 55.
(33) Densmore, D., Hsiau, T. H., Kittleson, J. T., DeLoache, W., Batten, C., and Anderson, J. C. (2010) Algorithms for automated DNA assembly. *Nucleic Acids Res. 38*, 2607−2616.
(34) Leguia, M., Brophy, J., Densmore, D., and Anderson, J. C. (2011) Automated assembly of standard biological parts. *Methods Enzymol. 498*, 363−397.
(35) Bennett, M. R., and Hasty, J. (2009) Microfluidic devices for measuring gene network dynamics in single cells. *Nat. Rev. Genet. 10*, 628−638.
(36) Kosuri, S., Eroshenko, N., Leproust, E. M., Super, M., Way, J., Li, J. B., and Church, G. M. (2010) Scalable gene synthesis by selective amplification of DNA pools from high-fidelity microchips. *Nat. Biotechnol. 28*, 1295−1299.
(37) Huang, M. C., Ye, H., Kuan, Y. K., Li, M. H., and Ying, J. Y. (2009) Integrated two-step gene synthesis in a microfluidic device. *Lab Chip 9*, 276−285.
(38) Kong, D. S., Carr, P. A., Chen, L., Zhang, S., and Jacobson, J. M. (2007) Parallel gene synthesis in a microfluidic device. *Nucleic Acids Res. 35*, e61.
(39) Cheng, W., Klauke, N., Smith, G., and Cooper, J. M. (2010) Microfluidic cell arrays for metabolic monitoring of stimulated cardiomyocytes. *Electrophoresis 31*, 1405−1413.
(40) Ahn, B., Lee, K., Lee, H., Panchapakesan, R., Xu, L., Xu, J., and Oh, K. W. (2011) Guiding, distribution, and storage of trains of shape-dependent droplets. *Lab Chip 11*, 3915−3918.
(41) Joensson, H. N., and Andersson Svahn, H. (2012) Droplet microfluidics—a tool for single-cell analysis. *Angew. Chem., Int. Ed. 51*, 12176−12192.
(42) Eastburn, D. J., Sciambi, A., and Abate, A. R. (2014) Identification and genetic analysis of cancer cells with PCR-activated cell sorting. *Nucleic Acids Res. 42*, e128.
(43) Sciambi, A., and Abate, A. R. (2014) Generating electric fields in PDMS microfluidic devices with salt water electrodes. *Lab Chip 14*, 2605−2609.
(44) Trivedi, V., Doshi, A., Kurup, G. K., Ereifej, E., Vandevord, P. J., and Basu, A. S. (2010) A modular approach for the generation, storage, mixing, and detection of droplet libraries for high throughput screening. *Lab Chip 10*, 2433−2442.
(45) Choi, K., Ng, A. H., Fobel, R., Chang-Yen, D. A., Yarnell, L. E., Pearson, E. L., Oleksak, C. M., Fischer, A. T., Luoma, R. P., Robinson, J. M., Audet, J., and Wheeler, A. R. (2013) Automated digital microfluidic platform for magnetic-particle-based immunoassays with optimization by design of experiments. *Anal. Chem. 85*, 9638−9646.
(46) Wheeler, A. R. (2008) Putting electrowetting to work. *Science 322*, 539−540.
(47) Shih, S. C. C., Mufti, N. S., Chamberlain, M. D., Kim, J., and Wheeler, A. R. (2014) A droplet-based screen for wavelength-dependent lipid production in algae. *Energy Environ. Sci. 7*, 2366−2375.
(48) Lafreniere, N. M., Shih, S. C., Abu-Rabie, P., Jebrail, M. J., Spooner, N., and Wheeler, A. R. (2014) Multiplexed extraction and quantitative analysis of pharmaceuticals from DBS samples using digital microfluidics. *Bioanalysis 6*, 307−318.
(49) Ng, A. H., Lee, M., Choi, K., Fischer, A. T., Robinson, J. M., and Wheeler, A. R. (2015) Digital microfluidic platform for the detection of rubella infection and immunity: a proof of concept. *Clin. Chem. 61*, 420−429.
(50) Abdelgawad, M., Watson, M. W., and Wheeler, A. R. (2009) Hybrid microfluidics: a digital-to-channel interface for in-line sample processing and chemical separations. *Lab Chip 9*, 1046−1051.
(51) Shih, S. C. C., Gach, P. C., Sustarich, J., Simmons, B. A., Adams, P. D., Singh, S., and Singh, A. K. (2015) A droplet-to-digital (D2D) microfluidic device for single cell assays. *Lab Chip 15*, 225−236.
(52) Watson, M. W., Jebrail, M. J., and Wheeler, A. R. (2010) Multilayer hybrid microfluidics: a digital-to-channel interface for sample processing and separations. *Anal. Chem. 82*, 6680−6686.
(53) Rival, A., Jary, D., Delattre, C., Fouillet, Y., Castellan, G., Bellemin-Comte, A., and Gidrol, X. (2014) An EWOD-based microfluidic chip for single-cell isolation, mRNA purification and subsequent multiplex qPCR. *Lab Chip 14*, 3739−3749.
(54) Au, S. H., Kumar, P., and Wheeler, A. R. (2011) A new angle on pluronic additives: advancing droplets and understanding in digital microfluidics. *Langmuir 27*, 8586−8594.
(55) Mazutis, L., Gilbert, J., Ung, W. L., Weitz, D. A., Griffiths, A. D., and Heyman, J. A. (2013) Single-cell analysis and sorting using droplet-based microfluidics. *Nat. Protoc. 8*, 870−891.
(56) Geng, T., Bao, N., Sriranganathanw, N., Li, L., and Lu, C. (2012) Genomic DNA extraction from cells by electroporation on an integrated microfluidic platform. *Anal. Chem. 84*, 9632−9639.
(57) Khine, M., Lau, A., Ionescu-Zanetti, C., Seo, J., and Lee, L. P. (2005) A single cell electroporation chip. *Lab Chip 5*, 38−43.
(58) Qu, B., Eu, Y. J., Jeong, W. J., and Kim, D. P. (2012) Droplet electroporation in microfluidics for efficient cell transformation with or without cell wall removal. *Lab Chip 12*, 4483−4488.
(59) Shih, S. C. C., Barbulovic-Nad, I., Yang, X., Fobel, R., and Wheeler, A. R. (2013) Digital microfluidics with impedance sensing for integrated cell culture and analysis. *Biosens. Bioelectron. 42*, 314−320.
(60) Shih, S. C. C., Fobel, R., Kumar, P., and Wheeler, A. R. (2011) A feedback control system for high-fidelity digital microfluidics. *Lab Chip 11*, 535−540.
(61) Lin, H. C., Liu, Y. J., and Yao, D. J. (2010) Core−shell droplets for parallel DNA ligation of an ultra-micro volume using an EWOD microfluidic system. *J. Lab. Autom. 15*, 210−215.
(62) Liu, Y. J., Yao, D. J., Lin, H. C., Chang, W. Y., and Chang, H. Y. (2008) DNA ligation of ultramicro volume using an EWOD microfluidic system with coplanar electrodes. *J. Micromech. Microeng. 18*, 045017.
(63) Au, S. H., Shih, S. C. C., and Wheeler, A. R. (2011) Integrated microbioreactor for culture and analysis of bacteria, algae and yeast. *Biomed. Microdevices 13*, 41−50.
(64) Kumar, P. T., Toffalini, F., Witters, D., Vermeir, S., Rolland, F., Hertog, M., Nicolai, B. M., Puers, R., Geeraerd, A., and Lammertyn, J. (2014) Digital microfluidic chip technology for water permeability measurements on single isolated plant protoplasts. *Sens. Actuators, B 199*, 479−487.
(65) Kuhnemund, M., Witters, D., Nilsson, M., and Lammertyn, J. (2014) Circle-to-circle amplification on a digital microfluidic chip for amplified single molecule detection. *Lab Chip 14*, 2983−2992.

DOI: 10.1021/acssynbio.5b00062
ACS Synth. Biol. 2015, 4, 1151−1164

(66) Hadwen, B., Broder, G. R., Morganti, D., Jacobs, A., Brown, C., Hector, J. R., Kubota, Y., and Morgan, H. (2012) Programmable large area digital microfluidic array with integrated droplet sensing for bioassays. *Lab Chip 12*, 3305−3313.
(67) Noh, J. H., Noh, J., Kreit, E., Heikenfeld, J., and Rack, P. D. (2012) Toward active-matrix lab-on-a-chip: programmable electrofluidic control enabled by arrayed oxide thin film transistors. *Lab Chip 12*, 353−360.
(68) Gong, J., and Kim, C. J. (2008) Direct-referencing two-dimensional-array digital microfluidics using multi-layer printed circuit board. *J. Microelectromech. Syst. 17*, 257−264.
(69) Jebrail, M. J., Renzi, R. F., Sinha, A., Van De Vreugde, J., Gondhalekar, C., Ambriz, C., Meagher, R. J., and Branda, S. S. (2015) A solvent replenishment solution for managing evaporation of biochemical reactions in air-matrix digital microfluidics devices. *Lab Chip 15*, 151−158.
(70) Cho, S., Kang, D. K., Sim, S., Geier, F., Kim, J. Y., Niu, X. Z., Edel, J. B., Chang, S. I., Wootton, R. C. R., Elvira, K. S., and deMello, A. J. (2013) Droplet-based microfluidic platform for high-throughput, multi-parameter screening of photosensitizer activity. *Anal. Chem. 85*, 8866−8872.
(71) Frenz, L., Blank, K., Brouzes, E., and Griffiths, A. D. (2009) Reliable microfluidic on-chip incubation of droplets in delay-lines. *Lab Chip 9*, 1344−1348.
(72) Koster, S., Angile, F. E., Duan, H., Agresti, J. J., Wintner, A., Schmitz, C., Rowat, A. C., Merten, C. A., Pisignano, D., Griffiths, A. D., and Weitz, D. A. (2008) Drop-based microfluidic devices for encapsulation of single cells. *Lab Chip 8*, 1110−1115.
(73) Weber, E., Engler, C., Gruetzner, R., Werner, S., and Marillonnet, S. (2011) A modular cloning system for standardized assembly of multigene constructs. *PLoS One 6*, e16765.
(74) Chang, C., Sustarich, J., Bharadwaj, R., Chandrasekaran, A., Adams, P. D., and Singh, A. K. (2013) Droplet-based microfluidic platform for heterogeneous enzymatic assays. *Lab Chip 13*, 1817−1822.
(75) Moon, T. S., Lou, C. B., Tamsir, A., Stanton, B. C., and Voigt, C. A. (2012) Genetic programs constructed from layered logic gates in single cells. *Nature 491*, 249−253.
(76) Goh, E. B., Baidoo, E. E., Burd, H., Lee, T. S., Keasling, J. D., and Beller, H. R. (2014) Substantial improvements in methyl ketone production in *E. coli* and insights on the pathway from in vitro studies. *Metab. Eng. 26C*, 67−76.
(77) Bokinsky, G., Peralta-Yahya, P. P., George, A., Holmes, B. M., Steen, E. J., Dietrich, J., Lee, T. S., Tullman-Ercek, D., Voigt, C. A., Simmons, B. A., and Keasling, J. D. (2011) Synthesis of three advanced biofuels from ionic liquid-pretreated switchgrass using engineered *Escherichia coli*. *Proc. Natl. Acad. Sci. U.S.A. 108*, 19949−19954.
(78) Zhang, Z., Zhao, P., Xiao, G., Watts, B. R., and Xu, C. (2011) Sealing SU-8 microfluidic channels using PDMS. *Biomicrofluidics 5*, 46503−465038.
(79) Shih, S. C. C., Yang, H., Jebrail, M. J., Fobel, R., McIntosh, N., Al-Dirbashi, O. Y., Chakraborty, P., and Wheeler, A. R. (2012) Dried blood spot analysis by digital microfluidics coupled to nano-electrospray ionization mass spectrometry. *Anal. Chem. 84*, 3731−3738.
(80) Ham, T. S., Dmytriv, Z., Plahar, H., Chen, J., Hillson, N. J., and Keasling, J. D. (2012) Design, implementation and practice of JBEI-ICE: an open source biological part registry platform and tools. *Nucleic Acids Res. 40*, e141.

DOI: 10.1021/acssynbio.5b00062
ACS Synth. Biol. 2015, 4, 1151−1164